

OPEN ACCESS

Relevance of Classical Models and Simulation Approaches for Battery Digital Twins

To cite this article: Tushar K. Telmasre *et al* 2025 *ECS Adv.* **4** 040503

View the [article online](#) for updates and enhancements.

You may also like

- [Review—Role of Nanomaterials in Screenprinted Electrochemical Biosensors for Detection of Covid-19 and for Post-Covid Syndromes](#)

Dola Sundeep, Eswaramoorthy K. Varadharaj, Kovuri Umadevi et al.

- [Electrochemical Performance of a Spatially Distributed ECPrOx Reactor](#)

Ivonne Karina Peña Arias, Richard Hanke-Rauschenbach and Kai Sundmacher

- [Semi-Analytical Methodology to Correct Polarization Curve to Measure Tafel Slope for an Electronic Resistance Laden Catalyst Layer](#)

Yadul Sethi, Yan-Sheng Li and Bharatkumar Suthar

Your Lab in a Box!

The PAT-Tester-i-16 Multi-Channel Potentiostat for Battery Material Testing!

EL-CELL®
electrochemical test equipment



- ✓ **All-in-One Solution with Integrated Temperature Chamber (+10 to +80 °C)!**
No additional devices are required to measure at a stable ambient temperature.
- ✓ **Fully Featured Multi-Channel Potentiostat / Galvanostat / EIS!**
Up to 16 independent battery test channels, no multiplexing.
- ✓ **Ideally Suited for High-Precision Coulometry!**
Measure with excellent accuracy and signal-to-noise ratio.
- ✓ **Small Footprint, Easy to Setup and Operate!**
Cableless connection of 3-electrode battery test cells. Powerful EL-Software included.

Learn more on our product website:



Download the data sheet (PDF):



Or contact us directly:

📞 +49 40 79012-734

✉️ sales@el-cell.com

🌐 www.el-cell.com



Relevance of Classical Models and Simulation Approaches for Battery Digital Twins

Tushar K. Telmasre,^{1,*} Aditya Naveen Matam,^{2,*} Chintan Pathak,³ Subhashini Sugumar,^{1,*} Lubhani Mishra,^{1,4,5,*} Bairav S. Vishnugopi,^{6,*} Partha P. Mukherjee,^{6,*} and Venkat R. Subramanian^{1,4,7,**,z}

¹Materials Science and Engineering, The University of Texas at Austin, Austin, Texas 78712, United States of America

²Chandra Department of Electrical Engineering, The University of Texas at Austin, Austin, Texas, 78712, United States of America

³BattGenie Inc., Seattle, Washington 98105, United States of America

⁴Walker Department of Mechanical Engineering, The University of Texas at Austin, Austin, Texas 78712, United States of America

⁵Allen J. Bard Center for Electrochemistry, The University of Texas at Austin, Austin, Texas 78712, United States of America

⁶School of Mechanical Engineering, Purdue University, West Lafayette, Indiana 47907, United States of America

⁷Affiliate Faculty, Oden Institute for Computational Science and Engineering, The University of Texas at Austin, Austin, Texas 78712, United States of America

Digital twins are virtual replicas of physical systems updated real time and are increasingly vital for complex systems like batteries. Being electrochemical black boxes that degrade with use, batteries benefit from digital twins for monitoring, predictive maintenance, and optimization. Data-driven models are popular for digital twins due to their adaptability, but are limited by dependence on large datasets, weak interpretability, and poor generalization. In contrast, physics-based approaches such as Pseudo-2D (P2D) models offer higher accuracy, interpretability, and require less operational data. These models can be packaged and deployed across platforms using the Functional Mock-up Interface (FMI) and Functional Mock-up Units (FMUs). Through FMU deployment, this paper illustrates the challenges and opportunities in balancing model depth and scale across battery chemistries, as well as the robustness and efficiency of numerical methods across spatial and temporal scales. In addition, the paper highlights how classical models already integrate data-driven elements, such as empirical fits for open-circuit voltage and electrolyte properties. The most effective digital twin strategies for batteries are therefore hybrid models that combine the rigor of physics-based methods with the flexibility of data-driven tools. Such interpretable, scalable, and fast models are essential for advancing energy storage and enabling real-time control in diverse applications.

© 2025 The Author(s). Published on behalf of The Electrochemical Society by IOP Publishing Limited. This is an open access article distributed under the terms of the Creative Commons Attribution 4.0 License (CC BY, <https://creativecommons.org/licenses/by/4.0/>), which permits unrestricted reuse of the work in any medium, provided the original work is properly cited. [DOI: [10.1149/2754-2734/ae213f](https://doi.org/10.1149/2754-2734/ae213f)]



Manuscript submitted September 15, 2025; revised manuscript received November 8, 2025. Published December 2, 2025.

Digital twin has become a popularly researched concept in the field of computations and modeling coupled together with real world applications. While Dr. Michael Grieves first conceptualized the idea for manufacturing in 2002, Digital Twin, as an official terminology, was first used by the Materials and Process Laboratory at NASA's Marshall Space Flight Center in 2010.^{1,2} A digital twin is a virtual, software-based representation of a physical asset, system, or process that accurately reflects its real-world counterpart throughout its lifecycle. Continuously updated with real-time data, it leverages simulation, machine learning, analytics, and reasoning to detect issues, predict outcomes, optimize performance, and support informed decision-making ultimately delivering measurable business value.^{3,4} In principle, the concept bridges the physical and digital worlds, establishing a continuous feedback loop in which data collected from sensors refines the virtual model, and the updated model informs interventions in the physical system. This dynamic exchange of information is what fundamentally differentiates digital twins from traditional static models.

Dr. Karen Wilcox, Director of the Oden Institute at UT Austin, has explained here⁵ that we are surrounded by powerful miniature computers in the form of smartphones, smartwatches, and health and wellness devices that are constantly collecting various types of data. Simultaneously, these devices run sophisticated models on the device or in the cloud that are rooted in physics and advanced statistics. Essentially, they continuously gather data about their users and build a virtual digital profile. For example, smartwatches collect health data on key indicators and use it to generate personalized suggestions and recommendations about our health and well-being.

What's more, as we age, our body composition changes, so what worked for us before may no longer be effective, hence the digital model reorients and adapts to these changing conditions. This is the essence of a digital twin, i.e., a virtual replica of a physical system that enables real-time monitoring, simulation, and optimization throughout the lifecycle of its subject. Such examples highlight how digital twins can enable interventions and optimize decision-making at both the individual and industrial scales.

Digital twins are widely used in a multitude of fields today. Apart from personal health, they are useful in the aerospace industry for aircraft design and maintenance; NASA famously used a digital twin of the Apollo 13 spacecraft to study the malfunctioning components and bring the stranded astronauts safely back home.¹ Another use for digital twins is in the launch and upkeep of satellites where they help in simulating flight behavior, orbital tracking and environmental control. On a larger scale, weather forecasting agencies have developed a digital twin of the whole Earth to monitor the weather patterns, track carbon cycles, water cycles/floods and currents in the oceans to provide real time weather data. More recently, industrial sectors such as automotive manufacturing and smart cities have adopted digital twins to improve sustainability, enhance safety, and enable predictive maintenance at scale. With the advent of newer physics-based and data-driven models, digital twins are slowly becoming omnipresent and affecting all aspects of engineering endeavors we know today.

Battery Models and Digital Twins

Batteries are electrochemical systems that only provide voltage and current as output measurements (in typical environments). Therefore, mathematical models of various levels of complexity are developed to study and predict internal processes and external outputs from the batteries.⁶⁻⁸ Batteries also degrade over time,

*Electrochemical Society Member.

**Electrochemical Society Fellow.

^zE-mail: venkat.subramanian@utexas.edu

changing their internal composition and capacity to hold charge. Thus, creating a digital twin of a battery system is essential to continually monitor and enhance its operational performance. A key guideline is that digital twins should not be treated as static representations. Rather, they must evolve alongside the battery, continuously incorporating new data to improve predictive accuracy over its lifetime. Recent papers by Dubarry and Howey provide an overview on the various scales at which battery digital twins can exist.^{3,9}

Digital twins of batteries rely on accurate and adaptable battery models to simulate, monitor, and predict the behavior of real-world battery systems under various operating conditions. These models act as the core analytical engine within the twin, allowing it to mirror the physical battery's internal states and performance in real-time. Battery models enable a digital twin to (a) Estimate State of Charge (SOC) and State of Health (SOH) with greater accuracy, (b) Predict thermal behavior, capacity fade, and internal resistance growth over time, (c) Optimize charging strategies and usage patterns to prolong battery life, (d) Provide early warnings for potential failures or unsafe conditions through fault detection and predictive maintenance, (e) Simulate various "what-if" scenarios to inform design or operational decisions, especially in electric vehicles (EVs), satellites, and grid energy storage. This functionality transforms battery management into a proactive and predictive framework, ensuring improved performance and reliability. A well-designed digital twin of a battery has applications across industries such as electric vehicles to help manage complex battery packs, detect cell imbalances, and support warranty analytics. In aerospace, battery digital twins ensure mission readiness and safety under extreme conditions. In stationary grid storage, they assist in real-time control, and degradation tracking.

On an individual cell level, battery models generally fall into these categories⁶

1. Equivalent Circuit Models (ECMs): They are simplified electrical analogs representing batteries using resistors, capacitors, and voltage sources. They are fast and computationally efficient, ideal for embedded systems and real-time applications but limited in capturing aging effects.
2. Electrochemical Models: They are based on many levels of physics-based electrochemical models differentiated on length scales. They involve partial differential equations (PDE)/differential algebraic equations (DAE) based mathematical description of electrochemical phenomena representing changes in mass transfer and interfacial reactions in batteries. Electrochemical models offer high accuracy often requiring greater computational resources.
3. Data-Driven & Hybrid Models: They combine machine learning with physics-based principles to handle complex patterns in battery behavior, improving adaptability while maintaining physical interpretability. Their strength lies in leveraging real-world data while retaining the robustness and explanatory power of physics-based models.

Each type of battery model has their strengths and weaknesses. Equivalent circuit models, though efficient in replicating battery behavior with their use of electrical circuit elements as equivalent electrochemical components within batteries, suffer from inherent empirical nature with no direct correlation with the physical processes occurring within the battery.¹⁰ Data driven models are the newer age entrants in the predictive modeling space that leverage advanced statistical models transformed into machine learning tools to predict battery behavior. Data driven machine learning models have been used in aspects such as parameters estimation,¹¹ battery aging models,¹²⁻¹⁴ safety and thermal management,¹⁵ predicting remaining useful life and so on. However, as the name suggests, these models need data which can prove to be a major pitfall in their predictive capabilities and usefulness. Further, owing to the nature of the production process of commercial batteries, there is significant cell to cell variability when it comes to performance of the batteries.

Thus, data-driven analysis performed on one type of battery won't necessarily directly translate into accurate prediction for a different type of battery or worse, similar battery from a different batch. With significant innovation happening in battery space every day, battery chemistry and design parameters are trade secrets for OEMs and not much of the data is shared across or released in the public domain. As a result, building generalized and transferable models remains a persistent challenge for data-driven approaches.

Data quality is another issue, as noisy, inconsistent, and poorly labeled data leads to unreliable models. Lack of physical interpretability is another major concern. While data-driven models may seem attractive when they provide accurate results, they essentially work like black boxes where the reasoning behind predictions can be obscure. Therefore, limitations such as data scarcity, overfitting, biases in training sets, and poor interpretability hinder the widespread adoption of purely data-driven models in safety-critical applications.

In this context, physics-based electrochemical models have proved their usefulness and reliability for both long-timescale academic research and fast-turnaround Battery Management System (BMS) applications.^{6,16} Figure 1 shows the hierarchy of battery models ranging from cell level Equivalent Circuit Models to atomistic simulations. Significant work has been carried out for the order reduction of the battery models that make them useful in fast parameter estimation, deployable in real time battery simulations and overall computational efficiency. An attractive part of physics-based models is the aspect of physical interpretability where change in model results can be traced back to physical changes to electrochemical components and reactions within the battery. Thus, in the space of digital twins, physics-based models are valuable in the following aspects.

1. Low data dependency: Since these models are grounded in physical laws, they require only material and cell parameters and not extensive operational data to make predictions. This is especially advantageous in early development stages or for novel chemistries where data is sparse.
2. Rich state estimation: Physics-based models can infer internal states of the battery (e.g., lithium concentration gradients, temperature fields, SEI layer growth) that are not directly measurable but are critical for health estimation and control.
3. Generalization across conditions: These models can be adapted to simulate a wide range of operating scenarios (different C-rates, temperatures, or cycling profiles) without retraining (or with reduced retraining), making them robust for real-world deployment.
4. Scenario planning and prognostics: Digital twins powered by physics models can perform "what-if" simulations, forecasting future states under varying usage, which is critical for predictive maintenance and lifecycle optimization.
5. Hybridization potential: Even when some data is available, hybrid models can be built by combining physics-based models with machine learning to correct residual errors or adapt to degradation over time.

Now that models have been briefly introduced, next we discuss taking these models to applications as digital twins.

Functional Mock-up Interface (FMI) for Battery Model Deployment

The Functional Mock-up Interface (FMI) is an open standard developed to enable the exchange and integration of dynamic models across different simulation tools.^{17,18} It defines a vendor- and tool-neutral API for packaging compiled simulation models including their equations, solver routines, and platform-specific libraries into a single, self-contained archive called a Functional Mock-up Unit (FMU). This standardized format ensures consistent behavior and results across operating systems and tools, simplifying model reuse, accelerating development, and streamlining collaboration.

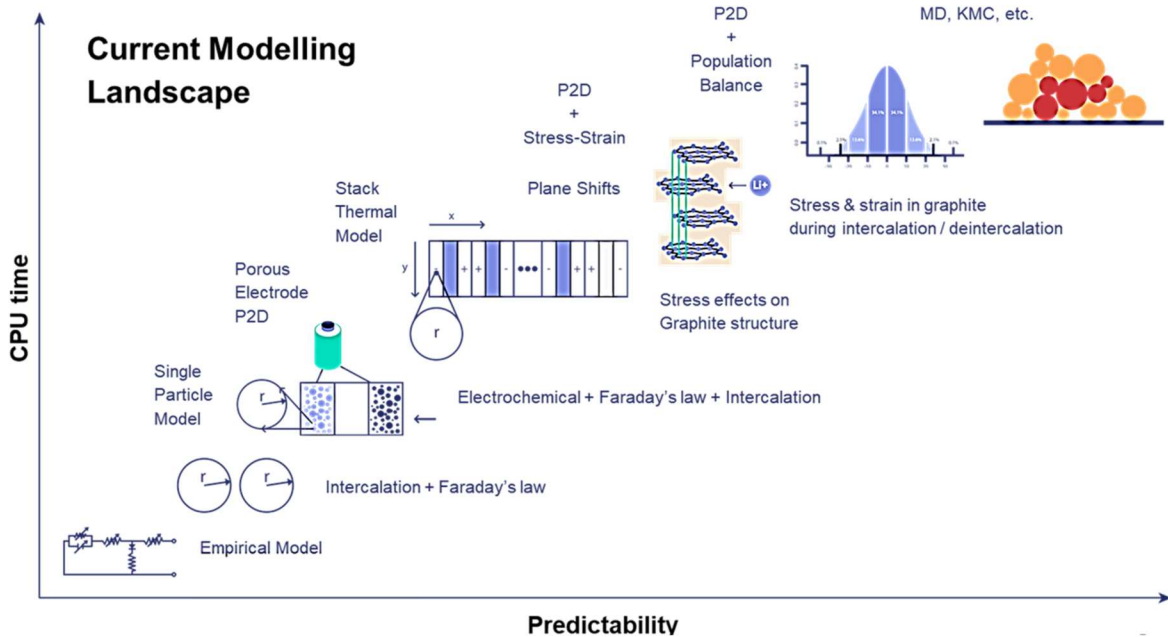


Figure 1. Hierarchy of battery models ranging from cell level Equivalent Circuit Models to atomistic simulations.

In the context of battery modeling, FMUs are especially powerful. Researchers and engineers can encapsulate high-fidelity physics-based models such as Single Particle Models (SPM), Open Circuit Voltage (OCV) models, phase field models, or thermal-electrochemical degradation models into modular black box components. These models can then be seamlessly integrated into larger system-level simulations for applications like BMS testing, component optimization, and digital twin deployments. The idea of FMU is to provide the user (especially experimental researchers and system level integrators (for EVs, grids)) with a tool that can readily provide model output without getting into details of the model equations. FMU-based battery models described here are developed in C++ and possess remarkable flexibility in input and output configurations. Therefore, a model can easily be built that accepts not only the input parameters from the experiments but also experimental data to perform validation. Figure 2 shows the salient features of battery functional mockup unit (FMU).

Black Box Paradigm

FMUs behave like opaque components under a strict input/output handshake paradigm:

- **Encapsulation:** All internal code, numerical solvers, and platform-specific libraries are hidden behind a standardized interface, protecting intellectual property and simplifying dependency management.
- **Interface Specification:** Each FMU exposes only a defined set of inputs (e.g., current profiles, temperature schedules) and outputs (e.g., surface/center concentration, OCV), along with tunable parameters.
- **Interoperability:** FMUs generated from different tools can be swapped or coupled within a simulation framework without requiring source code access or recompilation of the host application.

Execution Workflow:

1. **Prepare Inputs:** Populate a CSV file (e.g., lco-ocv_input_params.csv) with time-series and parameter values.
2. **Invoke Runner:** Execute the FMU runner (fmusim.exe) via command line, specifying the FMU file, input CSV, simulation start/stop times, output CSV path, and logging interval.

BATTERY FMU FEATURES

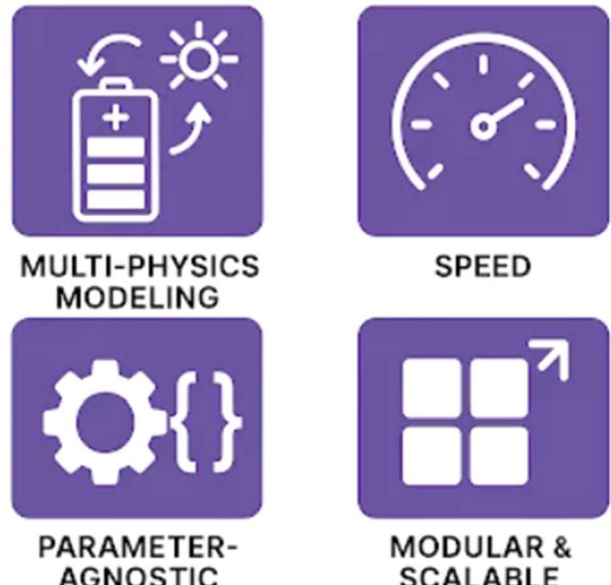


Figure 2. Battery functional mockup unit (FMU) features.

```
fmusim.exe \
--start-time 0 \
--stop-time 3600 \
--input-file lco-ocv_input_params.csv \
--output-file lco-output.csv \
--output-interval 10 \
\lco-ocv.fmu
```

3. **Post-Process Outputs:** Import the generated CSV (e.g., lco-output.csv) into analysis tools for visualization and further data-driven tuning.

Advantages

- **Portability:** One FMU runs identically across platforms and tools.

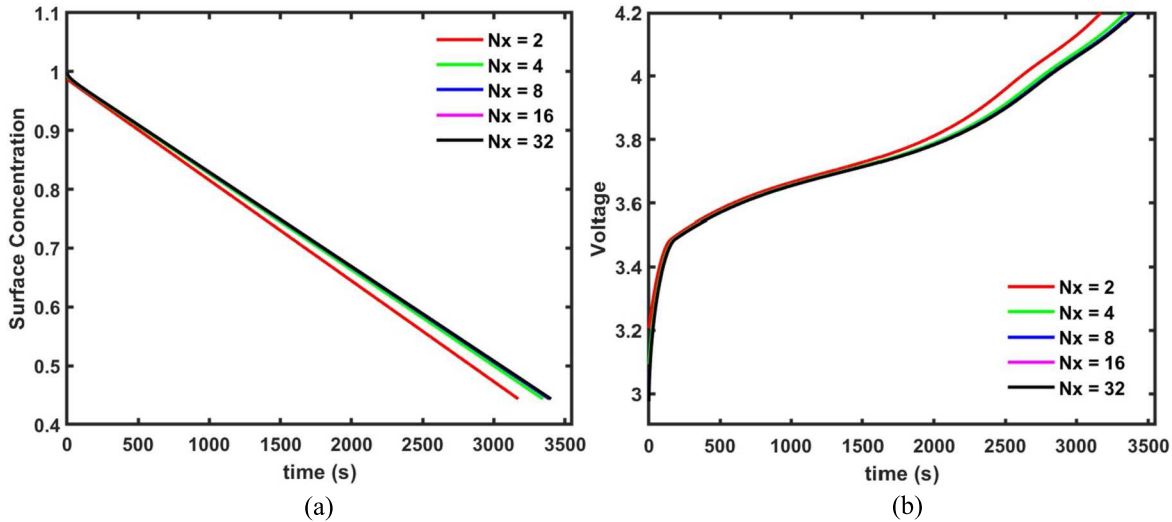


Figure 3. (a) Concentration at $x = 1$ vs time and (b) Voltage vs time plot for increasing number of node points ($N_x = 2, 4, 8, 16$, & 32) showing convergence after 8 node points. The discretization scheme used was cell centered finite difference. One can perform detailed error analysis for different applied currents to confirm that higher applied currents need a greater number of elements for convergence.

- Modularity: Plug-and-play architecture allows rapid model comparison and scalable system simulations.
- Abstraction: Users never need to compile or link source code, and proprietary implementations remain protected.
- Scalability & Efficiency: Algorithmically optimized FMUs support multi-physics modeling and parameter-agnostic performance, enabling system-level analysis under diverse loading and thermal conditions.

Trade-offs:

- Opacity: Internal solver settings and numerical methods are hidden, limiting opportunities for fine-grained debugging or customization.
- Runtime Overhead: The standardized FMI layer may introduce modest performance penalties.
- Versioning Challenges: Evolving FMU formats or tooling changes can cause compatibility issues if not carefully tracked.

In summary, by enabling tool-agnostic, encapsulated deployment of detailed battery models, FMUs offer a reproducible and maintainable way to integrate digital twins across diverse electrification applications. Whether for fast prototyping or production-grade simulations, this standard ensures that high-fidelity models remain modular, interoperable, and platform-independent.

Mathematical description of representative battery models for FMUs.—Let us now look at the role of physics and math that goes into the development of an FMU. Consider a physics-based electrochemical model for an NMC cathode particle that is charged. We use empirical OCV curve reported in literature¹⁹ with cell-centered finite difference discretization for spatial variables.

$$\begin{aligned}
 t_d \frac{\partial c}{\partial t} &= -\frac{1}{x^2} \frac{\partial(x^2 N_x)}{\partial x} = \frac{\partial^2 c}{\partial x^2} + \frac{2}{x} \frac{\partial c}{\partial x} \\
 t &= 0; c(0, t) = 1 \\
 x &= 0, -\frac{\partial c}{\partial x} = N_x = 0 \\
 x &= 1, -\frac{\partial c}{\partial x} = N_x = \frac{iapp.R^2}{3(1-\epsilon).ctp.lp.F.D}
 \end{aligned} \quad [1]$$

In this model, c and x are dimensionless concentration and distance, t is dimensional time (s), and t_d is the diffusion time constant $\left(\frac{R^2}{D}\right)$. N_x

represents the flux of concentration. Figure 3 presents the surface concentration for increasing number of node points ($N_x = 2, 4, 8, 16$, & 32). The same model described above can be approached with a different mathematical approach such as Galerkin weak form derived using symmetric polynomials explained elsewhere.²⁰ Figure 4 presents surface concentration with 1, 2, 3, 4, 5 terms using this approach.

Batteries however differ in their behavior for different chemistries. For LFP batteries, a phase separation is observed upon intercalation, and the voltage profile is much flatter around 3.2–3.4 V. As shown in a recent paper,²¹ to tackle the phase separation dynamics phase field models have been proposed to describe the intercalation behavior in LFP type cathodes. Equation 2 shows the phase field model used for lithium intercalation in the cathode.

$$\begin{aligned}
 t_d \frac{\partial c}{\partial t} &= -\frac{1}{x^2} \frac{\partial(x^2 N_x)}{\partial x}; N_x = -c(1-c) \frac{\partial \mu}{\partial x} \\
 \mu &= \log\left(\frac{c}{1-c}\right) + \omega(1-2c) - \kappa \frac{\partial^2 c}{\partial x^2} \\
 t &= 0; c(0, t) = 0.999 \\
 x &= 0, \frac{\partial c}{\partial x} = 0; N_x = -c(1-c) \frac{\partial \mu}{\partial x} = 0 \\
 x &= 1, \frac{\partial c}{\partial x} = 0; N_x = -c(1-c) \frac{\partial \mu}{\partial x} \\
 &= \frac{iapp.R^2}{3(1-\epsilon).ctp.lp.F.D}
 \end{aligned} \quad [2]$$

Where, N_x refers to the modified flux expression. μ is the chemical potential, whereas ω and κ are the enthalpy of mixing per site and the gradient energy penalty coefficient in dimensionless form respectively.²² Figure 5 shows a typical charge profile for LFP chemistry where the concentration at $x = 0$ and $x = 1$ is plotted with respect to time for the values of $\omega = 3$. It should be noted that, the higher ω value represents the phase separating behavior whereas the lower ω value represents the single-phase behavior as presented here.²¹ Further, we have observed that, for this model, using higher-order weak form finite element or higher-order spectral methods do not result in faster convergence.

Next, a digital twin was developed for Li-S batteries (a conversion chemistry) originally developed by Kumaresan and White and has been studied in detail by others.^{23–25} Model equations are given in Eq. 3. A cell-centered finite difference model of Li-S was developed and discharge curves at different C-rates predicted are given in Fig. 6. With respect to Li-S cathodes, it is noted that mesoscale modeling has captured how the Li_2S precipitate morphology (e.g., film-like vs. fractal growth) affects the evolution of electrochemically active area (e.g., surface passivation) and pore-

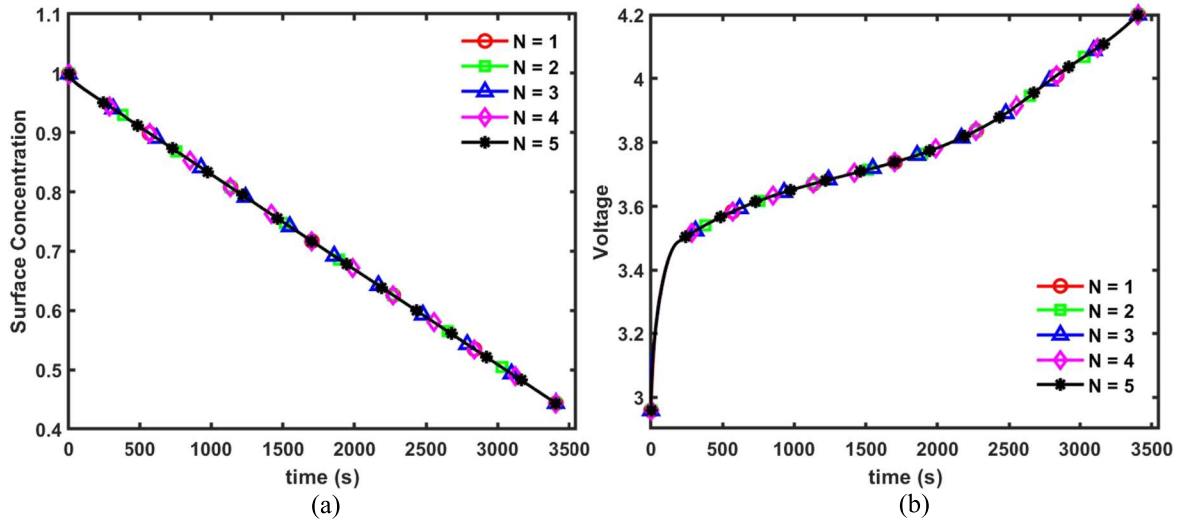


Figure 4. (a) Concentration at $x = 1$ vs time and (b) Voltage vs time plot for increasing number of terms ($N = 1, 2, 3, 4, \& 5$) for Galerkin weak form formulation using symmetric polynomials. Here, convergence is achieved after $N = 2$ indicating faster rate of convergence compared to the cell-centered finite difference discretization shown in Fig. 3.

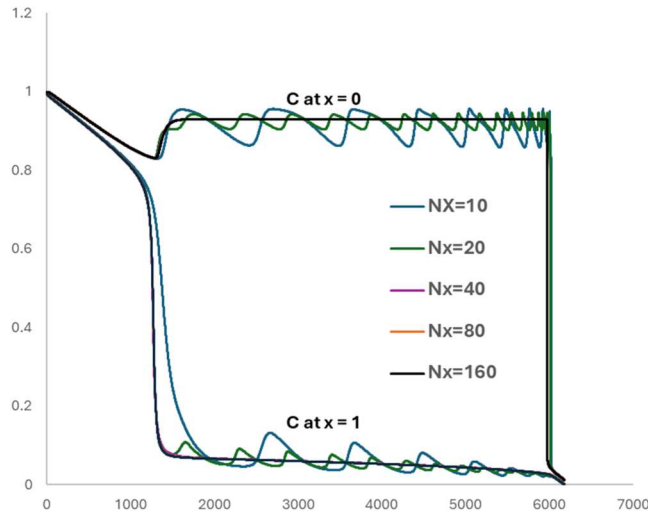


Figure 5. Concentration profile at $x = 0$ and $x = 1$ for LFP type phase separating electrodes during charging for $\omega = 3$.

phase transport, governing the shift from interface-limited to transport-limited regimes.^{26–28} In this context, pore-scale simulations enable the computation of effective electrode properties, including active area, pore-phase tortuosity, and electronic conductivity, that can be incorporated into cell-level performance models.²⁶ The development of microstructure-aware modeling frameworks is critical for accurately capturing how design parameters such as the electrolyte-to-sulfur (E/S) ratio, pristine porosity, pore size, and electrolyte transport properties affect cell performance and degradation pathways (e.g., polysulfide shuttle). Integrating such mesoscale models into digital twins allows dynamic microstructural evolution and associated electrochemical-transport interactions to be reflected in cell-level performance, thereby enhancing predictive fidelity and enabling earlier detection of degradation onset in Li-S batteries.

Governing Equations for Li-S model:²³

$$\frac{\partial eC_i}{\partial t} = -\nabla \cdot N_i + r_i - R_i$$

$$i_s = -\sigma \nabla \phi_1$$

$$i_e = F \sum z_i N_i$$

$$\nabla \cdot i_s + \nabla \cdot i_e = 0$$

where,

$$\begin{aligned} \frac{N_i}{\varepsilon} &= -D_i \nabla \cdot C_i - z_i \left(\frac{D_i}{RT} \right) F C_i \nabla \phi_2 \\ r_i &= -a \sum_j \frac{s_{i,j} i_j}{n_j F} \\ R_i &= \sum_k \gamma_{i,k} R'_k \\ R'_k &= k_k \varepsilon_k \left(\prod_i C_i^{\gamma_{i,k}} - K_{sp,k} \right) \\ \frac{\partial e}{\partial t} &= - \sum_k \tilde{V}_k R'_k \end{aligned}$$

$$x = 0, N_i = 0; -\sigma \nabla \phi_1 = I_{app}$$

$$x = L_p, N_{i,separator} = N_{i,cathode}; -\sigma \nabla \phi_1 = 0$$

$$x = L_p + L_s, N_1 = \frac{I_{app}}{F}; N_{i \neq 1} = 0; \phi_2 = 0 \quad [3]$$

Here, i represents the individual species taking part in electrochemical transport reactions, k represents solid phase species taking part in precipitation reactions. C_i is the concentration of species i and ε is the porosity. N_i represents the flux of species i . r_i and R_i represents rate of production/consumption of species i via electrochemical or precipitation reactions respectively. i_s represents solid phase current density and i_e represents liquid phase current density. a is interfacial surface area. D_i is diffusivity, $s_{i,j}$ is stoichiometric coefficient, $\gamma_{i,j}$ is number of moles of ionic species i in solid species k . k_k is rate constant and $K_{sp,k}$ is the solubility product for a precipitation reaction involving k . \tilde{V}_k is the partial molar volume of k and R'_k is the precipitation rate.

In this context, pore-scale simulations enable the computation of effective electrode properties, including active area, pore-phase

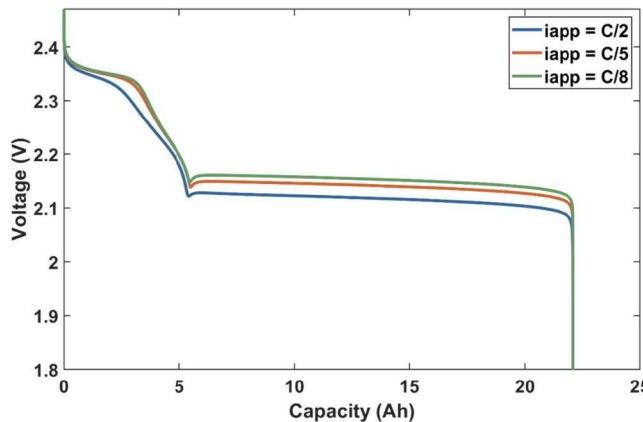


Figure 6. The typical discharge curve for Li-S model for different C-rates of C/2, C/5 and C/8.

tortuosity, and electronic conductivity, that can be incorporated into cell-level performance models.²⁶ The development of microstructure-aware modeling frameworks is critical for accurately capturing how design parameters such as the electrolyte-to-sulfur (E/S) ratio, pristine porosity, pore size, and electrolyte transport properties affect cell performance and degradation pathways (e.g., polysulfide shuttle). Integrating such mesoscale models into digital twins allows dynamic microstructural evolution and associated electrochemical-transport interactions to be reflected in cell-level performance, thereby enhancing predictive fidelity and enabling earlier detection of degradation onset in Li-S batteries.

To capture the influence of microstructure on transport behavior, the effective properties like tortuosity, electronic conductivity, and specific active surface area are evaluated using Direct Numerical Simulations (DNS), as discussed below.^{7,29} Microstructural inputs are generated by procedurally growing precipitates within an initially pristine mesoporous carbon scaffold, followed by evaluating transport properties on the resulting voxelized geometry. The scaffold is characterized by its initial porosity (ε_0), mean pore radius (R_p), and a representative elementary volume (REV) that has been pre-validated for both size and resolution independence. Precipitation is allowed to occur along carbon-pore and precipitate-pore interfaces, with local attachment influenced by a morphology factor (ω). Interfacial sites are prioritized for growth based on a defined deposition metric. At each growth increment, deposition sites are filled, and the interfacial areas are recalculated. These growth and characterization steps are iteratively repeated until the desired precipitate fraction is achieved. The directional pore tortuosity (τ_x , τ_y , τ_z) is then determined by solving the steady-state diffusion equation within the pore domain.

The steady state concentration balance is solved in the pore phase:

$$\nabla \cdot (D \nabla C) = 0 \quad [4]$$

The flux-equivalence relation in the following relation:

$$-D \frac{\varepsilon}{\tau_x} \left(\frac{C(x_{right}) - C(x_{left})}{x_{right} - x_{left}} \right) = - \int_{x=x_{left}} D \frac{\partial C}{\partial x} dy dz \\ = - \int_{x=x_{right}} D \frac{\partial C}{\partial x} dy dz \quad [5]$$

Which yields $\frac{\varepsilon}{\tau}$ along the chosen axis, and the same procedure is repeated for the other two directions to capture anisotropy, with isotropic averages reported when appropriate.

Effective electronic conductivity of the connected carbon network ($\sigma_{eff,x}$, $\sigma_{eff,y}$, $\sigma_{eff,z}$) is computed by solving charge conservation in the solid phase while treating pores and precipitate as insulators.

$$\nabla \cdot (\sigma \nabla \phi) = 0 \quad [6]$$

The directional effective conductivity then follows from.

$$-\sigma_x^{eff} \frac{\varepsilon}{\tau_x} \left(\frac{\phi(x_{right}) - \phi(x_{left})}{x_{right} - x_{left}} \right) = - \int_{x=x_{left}} \sigma \frac{\partial \phi}{\partial x} dy dz \\ = - \int_{x=x_{right}} \sigma \frac{\partial \phi}{\partial x} dy dz \quad [7]$$

In general, the effective electronic conductivity (σ_{eff}) closely follows the carbon fraction and remains nearly constant until the system approaches the percolation threshold. In contrast, the τ is highly sensitive to the ε_0 , R_p , precipitate volume fraction, and ω , as precipitation alters and constricts ionic transport pathways within the electrolyte. The validity of these formulations has been confirmed in previous studies.^{26,30,31} Table I provides microstructural properties as a function of various geometrical and morphological parameters described here.

Black boxing battery models—from simulation to estimation/optimization.—In this work, simulations were conducted for both identical models using different numerical discretization approaches, and different models using the same spatial discretization approach. For the model described here, the time integrator IDA (Implicit Differential-Algebraic equation solver) from the SUNDIALS (SUite of Nonlinear and DIfferential/ALgebraic equation Solvers)³² suite was found to be sufficiently robust and efficient for all simulations. Electrochemical battery models are stiff, highly nonlinear, ill-conditioned and require consistent initialization due to their inherent DAE nature. A discussion on consistent initialization of DAE models can be seen in.^{33,34} Stiffness in such systems is typically handled using implicit time solvers. Among available solvers, SUNDIALS's IDA has remained one of the most robust and efficient options, as demonstrated through decades of national laboratory testing. It is recommended to restrict the solver to

Table I. Mathematical correlation of microstructural properties as function of precipitation amount (ε_2), morphology (ω) and porosity (ε).

Property	Mathematical relation	Coefficient of determination, R^2
Active area (carbon-electrolyte interface)	$a = \frac{1}{R_p} (0.194794 + 4.636493(1 - \varepsilon_0) - 6.299025(1 - \varepsilon_0)^2) \left(1 - \left(\frac{\varepsilon_2}{0.247642 + 0.508887\omega^{2.862174}} \right) \right)^{0.171546}$	0.985191
Tortuosity	$\tau = (0.841432 - \varepsilon_2) (0.582207 + 0.829378\varepsilon_2 - 0.121772\omega)$	0.968584
Conductivity	$\sigma = 1.480809\sigma_0(1 - \varepsilon_0)^{2.130685}$	0.983681

a maximum order of 2, since the algorithm is not A-stable beyond that.³⁵ The nonlinearity of electrochemical battery models necessitates a robust Newton–Raphson solver, which in turn requires an analytic Jacobian for convergence. When numerical differentiation methods for computing the Jacobian fail or become unstable, the use of analytical Jacobians, derived with the help of tools such as Maple, Mathematica, or AutoDiff, can greatly improve robustness.

The choice of linear solver within IDA also plays a critical role. The ill-conditioning introduced by Butler–Volmer (BV) kinetics demands a robust direct linear solver. For one-dimensional models, Newman’s BANDJ algorithm based on Thomas’s tridiagonal method offers an efficient solution strategy. The codes presented in this paper, as well as IDA implementations for 1D problems, perform effectively using either Gaussian elimination (dense matrix algebra) or banded solvers (arising from finite difference or finite element methods with a known bandwidth).

When extending from 1D to 2D and 3D models, the use of sparse direct solvers becomes necessary. Based on our testing, PARDISO³⁶ currently offers the best performance for such systems. However, interfacing IDA with these solvers is not straightforward. Tools like COMSOL provide built-in interfaces to PARDISO and employ implicit time-stepping methods for battery simulations. In contrast, iterative solvers generally perform poorly for electrochemical battery models. Future work from our group will focus on converting some of these 2D and 3D models into FMU form for enhanced flexibility and interoperability.

Now that a robust and efficient digital twin has been developed for simulation models, the natural next step is to create a digital twin for parameter and model estimation, using both experimental data and the previously developed models.

Parameter Estimation as Optimization Problem

In addition to standard least-squares fitting, parameter estimation can be formulated as an optimization problem. This approach is

important because, beyond fitting voltage–time curves, the estimated parameters must remain within physically meaningful limits to ensure accurate tracking of a battery’s real-time behavior (voltage, temperature etc.). Therefore, the upper and lower bounds, as well as any linear constraints on the parameters, are incorporated into the optimizer based on battery physics. Optimization strategies can be broadly classified into two main categories, as illustrated in Fig. 7a. The parameter estimation based on optimization can be solved using either indirect methods or direct methods. The indirect methods are based on Pontryagin maximum principle which was discovered mid-19th century when computational expense was high. This method provides best answer if one can successfully implement the same.³⁷ However, it becomes impractical or at least difficult for larger, nonlinear models with active inequality constraints on state variables due to their computational complexity. Direct methods, on the other hand, transform the infinite-dimensional optimization problem into a finite-dimensional one, making it more computationally tractable. These methods can be further divided into simultaneous and sequential strategies, which are discussed in the following sections.

Simultaneous optimization strategy.—The schematic of this approach is shown in Fig. 7b. The dynamic mathematical models are typically PDEs. Spatial discretization of these PDEs converts the system into DAEs, and further temporal discretization transforms the DAEs into a set of nonlinear algebraic equations (NAEs). A nonlinear programming problem (NLP) is then formulated to minimize a specific objective function, with the NAEs explicitly defined as nonlinear constraints, along with any relevant path constraints. This approach enables the solution of the nonlinear optimization problem while avoiding model failures.^{38,39} In the past, we have used large scale nonlinear optimizers’ model-based control

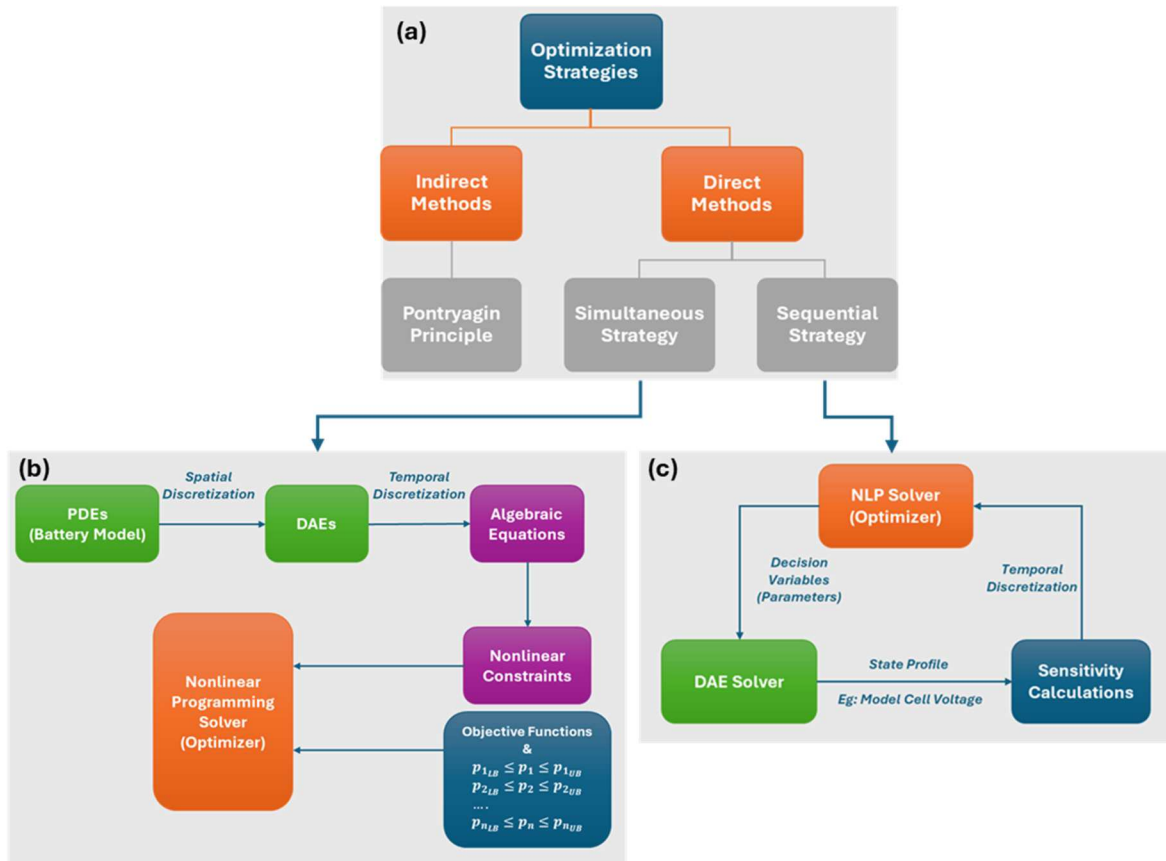


Figure 7. (a) Broad classification of various techniques that are used for parameter estimation (b) Simultaneous dynamic optimization strategy for parameter estimation (c) Sequential dynamic optimization strategy for parameter estimation.

strategies using physics-based battery model and for estimation of parameters. The primary challenge in this framework is the large number of time steps required for temporal discretization to achieve sufficient accuracy, as well as selecting an appropriate discretization strategy (e.g., collocation methods). As of today, only problems stated as algebraic equations (not PDEs or blackboxes) can be guaranteed to converge to global optima for convex problems. This makes the simultaneous approach attractive as it converts the optimization problem to a large set of algebraic equations.

Sequential optimization strategy.—The schematic of this approach is shown in Fig. 7c. In this strategy the DAE solver is integrated with NLP solver. At each iteration of the optimization cycle, the parameters (decision variables) are specified by the NLP solver. The solver simulates the model for the specific time period, or till a stop condition is achieved. The generated model simulation data is used to compute the objective function to generate parameters for the next iteration cycle. The optimization cycle will be continued till the objective function hits its minimum. This optimization strategy is robust when a DAE solver avoids model simulation failure. The FMUs developed in this paper enables researchers to solve optimization problems to estimate parameters without any error in optimization due to model simulation failure.⁴⁰ CASADI is very robust for optimization, but without proper initialization, calls to battery models within CASADI framework might fail. In addition, handling nonlinear path constraints is more challenging in the sequential approach as opposed to simultaneous approach.

Bayesian estimation can be viewed as a sequential approach for optimization, though it is not an optimization strategy. For example, in our past work,⁴¹ we had estimated five effective transport and kinetic parameters by applying least-squares estimation to experimental voltage-discharge data. The estimated parameters were the effective diffusion coefficient of lithium ion in the solution phase (D_1), effective diffusion coefficient of lithium in the solid phase for the negative and positive electrodes (D_{sn} and D_{sp}), and electrochemical reaction rate constants for the negative and positive electrodes (k_n and k_p). The effective negative-electrode solid-phase diffusion coefficient and reaction rate constant (D_{sn} and k_n) were found to decrease monotonically with cycles, whereas the other three parameters did not follow any trend. This suggested that the voltage-discharge curves may not contain sufficient information to accurately estimate the effective values of D_1 , D_{sp} , and k_p , resulting in large uncertainties in their values when fit only to experimental voltage-discharge curves.

Under-appreciated role of data-based approaches in classical models.—Even in the case of classical models, a significant point to note is the role of data-based approaches already embedded in them. The P2D model developed by Newman's group contains PDEs representing mass and charge transport coupled with electrode kinetics. The electrode OCV as a function of SOC is obtained using the data-based approaches only.¹⁶ The thermodynamics of intercalation is not fully predictable even today from physics-based approaches. Therefore, an OCP fit is obtained from experiments done on half cells. This fit, in the form of a piecewise polynomial or an empirical nonlinear mathematical function, is used to correctly obtain the voltage at individual electrodes. Thus, empirical fits from experimental data and numerical solution of classical PDEs are used for physics based electrochemical modeling of batteries for the last 3 decades.

Another application of data driven approaches in classical models is the electrolyte conductivity used in battery models. The conductivity of electrolytes is generally derived from independent data and applied as input to the P2D models. AI based approaches are making a difference in identifying electrolytes for improved conductivity.⁴² In addition, Bruggeman coefficient, which represents the tortuosity of the media, needs rethinking at the microscale. At that length scale, a 2D/3D model representation becomes important. Successful past efforts in microscale come from detailed numerical

simulation based on SEM images of a porous electrode and learning updated tortuosity, diffusion coefficients and local heterogeneity from offline simulation.

Future prospects and perspective.—The examples presented above were from approximate models such as SPM model simulated using spectral (Galerkin) and cell-centered finite difference method. It was shown that faster convergence is achieved by carefully selecting the numerical method to solve the model involved. For the description of mass and charge transport through all the three domains, i.e., cathode, anode and electrolyte; P2D models have proved themselves to be the gold standard in this space. An FMU has been developed by us for P2D models that show superior performance in various conditions up to 10x faster than commercially available software such as COMSOL. This has been licensed by an OEM. In addition, a digital twin has also been developed for Li-S batteries.

In the context of digital twins, the speed of the underlying model is critical to expedite faster analysis of possible scenarios for best predictions. Rapid simulation capabilities improve computational efficiency and make real-time decision support feasible, which is essential for large-scale applications such as EV fleets and grid energy storage. Using the best possible model and best possible algorithm helps us arrive at perhaps the fastest digital twin as elaborated in the previous section. A fast model also supports continuous monitoring and enables the twin to adapt dynamically to new conditions and operational realities. In addition, computational speed underpins advanced techniques such as Bayesian estimation and uncertainty quantification, which enhance robustness and reliability. This can enable better prediction of battery states and parameters, improve performance and support the development of optimal charging profiles.

In advancing the data driven and machine learning models applied to batteries, physics informed machine learning models for batteries are gaining popularity.⁴³ This helps with the interpretability and validation of the data driven models.

Our future work in this area also includes developments of FMUs for parameter estimation and Bayesian estimation to understand degradation and optimization to identify fast charging profiles. This will include estimation and optimal control approaches based on the combination of robust time integrators coupled with optimizers and estimators. Note that by brute forcing and by running a lot of simulations, robust optimization can be performed with Genetic Algorithms, simulated annealing, etc. However, gradient based approaches, if they work can be very efficient and can be implemented in real-time in embedded systems. As seen earlier, optimization codes can fail, if the model is not simulated to sufficient precision providing inaccurate gradients and Hessians. Also, active inequalities of very simple models can result in high index DAEs³¹ which cannot be even simulated today with standard packages or solvers without order reduction.

Conclusions

The future of battery research and development undoubtedly or at least partially lies in the adoption of digital twin technology. These virtual representations of batteries, built upon fundamental models, whether physics-based or data-driven, offer unprecedented opportunities for monitoring, control, and optimization. However, careful model selection remains crucial: the chosen model must strike the right balance between accuracy and computational efficiency to be practical and scalable. While data-driven models are gaining popularity, their shortcomings such as limited interpretability and dependence on large datasets cannot be overlooked. Hence, the most promising path forward involves developing hybrid models that are rooted in electrochemical fundamentals, judiciously integrate data-driven techniques, and remain computationally lightweight. This holistic approach holds the key to unlocking the full potential of digital twins for batteries, ultimately accelerating innovation and deployment in energy storage systems.

Code Dissemination

All the FMUs developed and presented in this paper (including the original source codes in C++) are available upon request from the corresponding author, Venkat R. Subramanian, without any restrictions.

Acknowledgments

The information, data, or work presented herein (for the modeling and simulation) was funded by the Office of Energy Efficiency and Renewable Energy (EERE), U.S. Department of Energy, under Award Number DE-EE0011166. The authors gratefully acknowledge the Allen J. Bard Center for Electrochemistry, University of Texas at Austin, for providing partial financial support for this work through the Bard CEC Student Scholar Fellowship under Grant no. H-F-0037 facilitated by the Welch Foundation.

ORCID

Tushar K. Telmasre  <https://orcid.org/0000-0002-7389-029X>
 Aditya Naveen Matam  <https://orcid.org/0009-0009-6611-6990>
 Chintan Pathak  <https://orcid.org/0000-0002-1480-0856>
 Subhashini Sugumar  <https://orcid.org/0009-0004-0744-7160>
 Lubhavni Mishra  <https://orcid.org/0000-0003-2135-9381>
 Bairav S. Vishnugoppi  <https://orcid.org/0009-0002-6357-9358>
 Partha P. Mukherjee  <https://orcid.org/0000-0001-7900-7261>
 Venkat R. Subramanian  <https://orcid.org/0000-0002-2092-9744>

References

1. NASA's Biological and Physical Sciences Division, (2021), <https://science.nasa.gov/biological-physical/why-does-the-world-and-nasa-need-digital-twins/>.
2. N. GallagherIBM, <https://ibm.com/think/topics/what-is-a-digital-twin> (2025).
3. M. Dubarry, D. Howey, and B. Wu, "Enabling battery digital twins at the industrial scale." *Joule*, **7**, 1134 (2023).
4. K. Wilcox and B. Segundo, "The role of computational science in digital twins." *Nat. Comput. Sci.*, **4**, 147 (2024).
5. TEDxUTAustin, K. Wilcox, (2022), https://ted.com/talks/karen_wilcox_how_digital_twins_could_help_us_predict_the_future.
6. V. Ramadesigan, P. W. C. Northrop, S. De, S. Santhanagopalan, R. D. Braatz, and V. R. Subramanian, "Modeling and simulation of lithium-ion batteries from a systems engineering perspective." *J. Electrochem. Soc.*, **159**, R31 (2012).
7. A. N. Mistry, K. Smith, and P. P. Mukherjee, "Secondary-phase stochastics in lithium-ion battery electrodes." *ACS Appl. Mater. Interfaces*, **10**, 6317 (2018).
8. B. S. Vishnugoppi, A. Verma, and P. P. Mukherjee, "Fast charging of lithium-ion batteries via electrode engineering." *J. Electrochem. Soc.*, **167**, 090508 (2020).
9. B. Wu, W. D. Widanage, S. Yang, and X. Liu, "Battery digital twins: perspectives on the fusion of models, data and artificial intelligence for smart battery management systems." *Energy and AI*, **1**, 100016 (2020).
10. N. Meddings et al., "Application of electrochemical impedance spectroscopy to commercial Li-ion cells: a review." *J. Power Sources*, **480**, 228742 (2020).
11. D. Roman, S. Saxena, V. Robu, M. Pecht, and D. Flynn, "Machine learning pipeline for battery state-of-health estimation." *Nat. Mach. Intell.*, **3**, 447 (2021).
12. Z. Nozarijouybari and H. K. Fathy, "Machine learning for battery systems applications: progress, challenges, and opportunities." *J. Power Sources*, **601**, 234272 (2024).
13. S. Harippriya, E. Esakkil Vigneswaran, and S. Jayanthi, "Battery management system to estimate battery aging using deep learning and machine learning algorithms." *J. Phys. Conf. Ser.*, **2325**, 012004 (2022).
14. V. Kabra, A. Karmakar, B. S. Vishnugoppi, and P. P. Mukherjee, "Quantifying the effect of degradation modes on Li-ion battery thermal instability and safety." *Energy Storage Mater.*, **74**, 103878 (2025).
15. A. Al Miaari and H. M. Ali, "Batteries temperature prediction and thermal management using machine learning: an overview." *Energy Reports*, **10**, 2277 (2023).
16. M. Doyle, T. F. Fuller, and J. Newman, "Modeling of galvanostatic charge and discharge of the lithium/polymer/insertion cell." *J. Electrochem. Soc.*, **140**, 1526 (1993).
17. L. I. Hatledal, A. Styve, G. Hovland, and H. Zhang, "A language and platform independent Co-simulation framework based on the functional mock-up interface." *IEEE Access*, **7**, 109328 (2019).
18. M. Elsotohy, J. Jaeschke, F. Sehr, and M. Schneider-Ramelow, "Mission profile-based digital twin framework using functional mock-up interfaces for assessing system's degradation behaviour." *Microelectron. Reliab.*, **150**, 115086 (2023).
19. A. Subramanian, S. Kolluri, C. D. Parke, M. Pathak, S. Santhanagopalan, and V. R. Subramanian, "Properly lumped lithium-ion battery models: a tanks-in-series approach." *J. Electrochem. Soc.*, **167**, 013534 (2020).
20. R. S. Thiagarajan et al., "Efficient reformulation of linear and nonlinear solid-phase diffusion in lithium-ion battery models using symmetric polynomials: mass conservation and computational efficiency." *J. Electrochem. Soc.*, **170**, 010528 (2023).
21. T. K. Telmasre et al., "Perspective—moving next-generation phase-field models to BMS applications: a case study that confirms professor Uzi Landau's foresight." *J. Electrochem. Soc.*, **171**, 063507 (2024).
22. Y. Zeng and M. Z. Bazant, "Phase separation dynamics in isotropic ion-intercalation particles." *SIAM J. Appl. Math.*, **74**, 980 (2014).
23. K. Kumaresan, Y. Mikhaylik, and R. E. White, "A mathematical model for a lithium–sulfur cell." *J. Electrochem. Soc.*, **155**, A576 (2008).
24. T. Zhang, M. Marinescu, S. Walus, and G. J. Offer, "Modelling transport-limited discharge capacity of lithium-sulfur cells." *Electrochim. Acta*, **219**, 502 (2016).
25. C. D. Parke, A. Subramanian, S. Kolluri, D. T. Schwartz, and V. R. Subramanian, "An efficient electrochemical tanks-in-series model for lithium sulfur batteries." *J. Electrochem. Soc.*, **167**, 163503 (2020).
26. A. Mistry and P. P. Mukherjee, "Precipitation–microstructure interactions in the Li–Sulfur battery electrode." *The Journal of Physical Chemistry C*, **121**, 26256 (2017).
27. A. N. Mistry and P. P. Mukherjee, "Electrolyte transport evolution dynamics in lithium–sulfur batteries." *The Journal of Physical Chemistry C*, **122**, 18329 (2018).
28. A. N. Mistry and P. P. Mukherjee, "Shuttle" in polysulfide shuttle: friend or Foe?" *The Journal of Physical Chemistry C*, **122**, 23845 (2018).
29. C.-F. Chen, A. Verma, and P. P. Mukherjee, "Probing the role of electrode microstructure in the lithium-ion battery thermal behavior." *J. Electrochem. Soc.*, **164**, E3146 (2017).
30. A. D. Dysart et al., "Towards next generation lithium-sulfur batteries: non-conventional carbon compartments/sulfur electrodes and multi-scale analysis." *J. Electrochem. Soc.*, **163**, A730 (2016).
31. S. L. Campbell, "High-index differential algebraic equations." *Mechanics of Structures and Machines*, **23**, 199 (1995).
32. A. C. Hindmarsh et al., "SUNDIALS." *ACM Transactions on Mathematical Software*, **31**, 363 (2005).
33. K. Shah et al., "Editors' choice—perspective—challenges in moving to multiscale battery models: where electrochemistry meets and demands more from math." *J. Electrochem. Soc.*, **167**, 133501 (2020).
34. M. T. Lawder, V. Ramadesigan, B. Suthar, and V. R. Subramanian, "Extending explicit and linearly implicit ODE solvers for index-1 DAEs." *Computers & Chemical Engineering*, **82**, 283 (2015).
35. E. Hairer and G. Wanner, "Examples of stiff equations." *Solving Ordinary Differential Equations II* (Springer, Berlin, Heidelberg) Series in Computational Mathematics, 14, 2 ed. (1996), https://doi.org/10.1007/978-3-642-05221-7_1.
36. M. A. Patterson and A. V. Rao, "GPOPS-II." *ACM Transactions on Mathematical Software*, **41**, 1 (2014).
37. L. T. Biegler, "New directions for nonlinear process optimization." *Curr Opin Chem Eng*, **21**, 32 (2018).
38. L. T. Biegler, "Multi-level optimization strategies for large-scale nonlinear process systems." *Comput. Chem. Eng.*, **185**, 108657 (2024).
39. J. A. E. Andersson, J. Gillis, G. Horn, J. B. Rawlings, and M. Diehl, "CasADI: a software framework for nonlinear optimization and optimal control." *Math Program Comput.*, **11**, 1 (2019).
40. V. Ramadesigan, K. Chen, N. A. Burns, V. Boovaragavan, R. D. Braatz, and V. R. Subramanian, "Parameter estimation and capacity fade analysis of lithium-ion batteries using reformulated models." *J. Electrochem. Soc.*, **158**, A1048 (2011).
41. C. Chen et al., "Accelerating computational materials discovery with machine learning and cloud high-performance computing: from large-scale screening to experimental validation." *J. Am. Chem. Soc.*, **146**, 20009 (2024).
42. S. Navidi, A. Thelen, T. Li, and C. Hu, "Physics-informed machine learning for battery degradation diagnostics: a comparison of state-of-the-art methods." *Energy Storage Mater.*, **68**, 103343 (2024).